

## VISUALISATION OF THE INTERACTION BETWEEN ACIDITHIOBACILLUS FERROOXIDANS AND OIL SHALE BY ATOMIC FORCE MICROSCOPY

**J. S. Milić<sup>\*,#</sup>, V.P. Beškoski<sup>\*</sup>, D. V. Randjelović<sup>\*\*</sup>, J. Stojanović<sup>\*\*\*</sup>, M. M. Vrvic<sup>\*,\*\*\*\*</sup>**

<sup>\*</sup>Department of Chemistry, Institute of Chemistry, Technology and Metallurgy,  
University of Belgrade, Studentski trg 12, 11000 Belgrade, Serbia

<sup>\*\*</sup>Department of Microelectronic Technologies and Single Crystals, Institute  
of Chemistry, Technology and Metallurgy, University of Belgrade,  
Studentski trg 12, 11000 Belgrade, Serbia

<sup>\*\*\*</sup>Faculty of Science, University of Kragujevac, Radoja  
Domanovica 12, 34000 Kragujevac, Serbia

<sup>\*\*\*\*</sup>Department of Biochemistry, Faculty of Chemistry, University  
of Belgrade, Studentski trg 12-16, 11000 Belgrade, Serbia

*(Received 23 September 2011; accepted 28 November 2011)*

---

### *Abstract*

*This study visually documents the mechanical contact and interaction between the bacterial cells of two biogeocentically different strains of *Acidithiobacillus ferrooxidans* (*At. ferrooxidans*) and oil shale containing pyrite. Atomic force microscopy (AFM) imaging was used to visualise initial interaction between the microorganisms and the surface minerals of an oil shale and to evaluate bacterial effects in the first hours of the bioleaching process. *Acidithiobacillus ferrooxidans* was attached to the shale surface already after 2 h, and after 48 h, numerous cells covered the surface with a biofilm. After 5 day incubation with *At. ferrooxidans*, AFM imaging revealed ellipsoid etched pits that represent footprints left by detached cells. Combining AFM surface imaging and leaching analysis following bacterial colonisation of oil shale layers demonstrates that an initial attachment to the surface is necessary for the leaching and that later on, once a sufficient concentration of  $Fe^{2+}$  ions in the solution is achieved, cells detach to become free cells, and leaching occurs primarily by*

---

<sup>#</sup> Corresponding author: [jelena\\_milic@yahoo.com](mailto:jelena_milic@yahoo.com)

the  $Fe^{3+}$ . This experiment confirmed that microorganisms isolated from sites in which a particular substrate is found will demonstrate stronger binding to that substrate.

*Keywords: Atomic force microscopy; Acidithiobacillus ferrooxidans; Bioleaching; Oil shale*

## 1. Introduction

Oil shale is a compact, homogenous, fine-grained sedimentary rock, often with a layered structure, and is potentially important as a source of energy i.e., as an alternative hydrocarbon fuel. Due to this potential oil shale is of economic interest and the subject of various geochemical investigations [1-4]. The majority of components in oil shale (approximately 80%) are inorganic, such as carbonates, aluminosilicates and pyrite ( $FeS_2$ ). Kerogen, insoluble in organic and inorganic solvents and of a heterogeneous macromolecular cross-linked structure, is the dominant organic substance (approximately 95% of the total organic matter). Regarding components soluble in organic solvents, bitumen accounts for a significant portion (commonly 5%), [5,6].

Pyrite interferes with kerogen degradation processes involving oxidants, and elemental analysis of the kerogen. Therefore, preparation of pure and unaltered kerogen concentrates is of interest. [7-9].

The most important mesophilic bacteria for the extraction of sulphide minerals such as pyrite are iron- and sulphur-oxidising *Acidithiobacillus ferrooxidans* (*At. ferrooxidans*), sulphur-oxidising *At. thiooxidans* and *At. caldus* and iron-oxidising *Leptospirillum* spp. (*L. ferriphilum* and *L. ferrooxidans*) [10-12]. An important characteristic of these bacteria is their ability

to interact with mineral surfaces [13], and following that process the cells produce extracellular polymeric substances (EPS) that stabilise this contact [14-19].

Most studies published to date on leaching ores have investigated the effects of oil shale properties on acid generation and bacterial bioleaching kinetics of sulphide ores, as well as the use of microorganisms for the selective separation of sulphide minerals [20-23].

This study is considered to be the first reported visualisation and mechanistic analysis of bacteria attaching to an oil shale substrate.

The aim of this study was to follow colonisation of oil shale containing pyrite ( $FeS_2$ ) after 2 h, 6 h, 12 h, 24 h, 48 h and 5 d of incubation with two different strains of *At. ferrooxidans* and evaluate bacterial attachment and bacterial effects in the first hours of bioleaching process. Atomic force microscopy (AFM) is used to visualise contact interactions between the microorganisms (bacterial attachment) and an oil shale surface and to determine initial interactions between bacteria cells and oil shale surface minerals in bioleaching process [24,25]. The AFM method requires minimal sample preparation and creates three-dimensional images in high resolution [26]. Topographic information from AFM images is acquired by scanning the surface with a sharp probe. Because the underlying interatomic tip-sample interaction forces are

on the order of  $10^{-7}$  N to  $10^{-6}$  N in the contact mode of operation, this AFM technique is applicable to a wide range of experimental studies, including biological samples [27].

## 2. Experimental

### 2.1 Preparation of oil shale substrate

Oil shale samples (approximately 1 mm thickness), which originated from the oil shale deposit near Aleksinac (Serbia), were prepared for the experiment by treatment with diluted hydrochloric acid (1:2, *m:V*) for 1 h at room temperature and 2 h at 50 °C in a water bath [28]. Subsequently, the oil shale samples were flushed with demineralised water until a negative reaction for chloride ions was achieved and then disinfected in 70% ethanol for 12 h, followed by rinsing with deionised water (Milli-Q® water system, Millipore; resistivity 18.2 MΩ cm, TOC < 10 µg l<sup>-1</sup>) and drying in a vacuum desiccator. Chemical analysis after HCl treatment showed that the oil shale contained 64.3% C, 8.3% H, 1.8% N, 13.0% FeS<sub>2</sub> and 58.2% ash. The X-ray diffraction (XRD) pattern for raw oil shale and the HCl-concentrate of oil shale is shown in Fig. 1.

### 2.2 Strains and inocula preparation

Pure cultures of the most active zymogenous strains of *At. ferrooxidans* [29] were isolated from specimens taken from two locations: an oil shale specimen taken from the old open pit mine near Aleksinac (Serbia) and acid mine drainage (AMD) waters from the copper-mine dump Bor (Serbia). Culturing and isolation have been

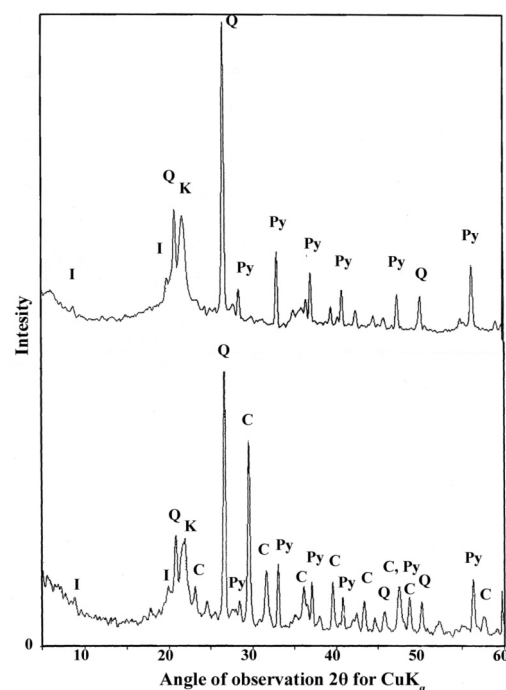


Fig. 1. XRD pattern of raw and HCl concentrate oil shale for the Aleksinac oil shale deposit. (Q: quartz, I: illite, K: cristobalite, Py: pyrite, C: calcite)

described elsewhere [30,31]. The two activated bacterial strains (*At. ferrooxidans* A, isolated from Aleksinac and *At. ferrooxidans* B, isolated from Bor) were separately prepared for the experiments with three successive reseedings in 500 ml Erlenmeyer flasks containing 100 ml of 9K medium [32] adjusted to pH 2.5 with sulphuric acid. The third reseedings were carried out in 5 l flasks that contained 1 l of 9K medium. All flasks were shaken using a rotary shaker with rotation and temperature set at 200 rpm and  $28 \pm 1$  °C, respectively. After five days, the bacterial cultures were filtered through 0.45 µm membrane filters, washed with 9K iron-free medium (OK) and subsequently resuspended in 120 cm<sup>3</sup> of OK medium. In this way, cell densities of up to 5

$\times 10^6$  cells/ml per flask were obtained.

The number of cells was determined by a Thoma chamber using a phase-contrast microscope [33].

### 2.3 Experimental design

The experiments were carried out in 500 ml Erlenmeyer flasks, each containing 100 ml of OK medium, 20 ml activated bacterial suspension (as described in section 2.2, with a final cell density per sample flask of  $9 \times 10^5$  cells/ml) and 10.00 g of oil shale (in the form of oil shale layers). The final ratio of oil shale layers (solid phase) and OK medium (liquid phase) was 1:12 (*m:V*). Prior to adding the OK medium, the shale layers were heated in the flasks to 80 °C for 1 h for sterilisation purposes [28]. An abiotic control flask also contained 120 ml of OK medium and 10.00 g oil shale and was treated under identical experimental conditions.

To obtain continuous leaching of samples with a constant ratio of oil shale to nutrient medium, the samples were prepared in such a way that at particular time points an entire flask was sacrificed for analysis [28].

The experiments were carried out for 5 days under stationary conditions at  $28 \pm 1$  °C, with periodic mixing. The progress of bioleaching was monitored in both the inoculated and control samples by measuring the pH, total pyrite bioleached,  $\text{Fe}^{2+}$  and  $\text{Fe}^{3+}$  concentrations in solution and by AFM imaging after 2 h, 6 h, 12 h, 24 h, 48 h and 5 d.

### 2.4 Chemical analyses

Elemental analysis was performed using a

CHNOS Elemental Analyzer, Vario EL III device (Hanau, Germany). The iron concentration was measured by atomic absorption spectrometry with a Perkin Elmer analyst model 1100B (Norwalk USA) and calculated to the pyrite concentration.

The relationship between  $\text{Fe}^{2+}$  and  $\text{Fe}^{3+}$  in solution was determined by measuring electromotive force (EMF) with a coiled platinum and saturated calomel electrode ( $\text{Hg}/\text{Hg}_2\text{Cl}_2/\text{Cl}^-$ ), on the basis of a calibration curve,  $\text{EMF} = f[\log(\text{Fe}^{3+}/\text{Fe}^{2+})]$ . Subsequently, the ratios of  $\text{Fe}^{3+}:\text{Fe}^{2+}$  were converted to absolute values on the basis of the total iron concentrations in the solutions.

The EMF and pH were measured using a mV/pH meter PHM220 (Radiometer, Copenhagen) with a Pt electrode (M21Pt), with saturated calomel REF401 as a reference electrode and a pH-combined electrode (PH2001-8), which were all obtained from the same manufacturer.

X-ray diffraction analysis was done using a Siemens diffraction spectrometer with a type F goniometer and a  $\text{CuK}_\alpha$  Ni-filtered radiation source. The results were interpreted by comparison with data from standard tables (Committee on Powder Diffraction Standards, 1974).

### 2.5 AFM instrumentation

The surface topography of the samples was observed by AFM. AFM characterisations were performed with an AutoProbe CP-Research SPM (TM Microscopes-Veeco) using a 90  $\mu\text{m}$  large-area scanner. Measurements were carried out in air using the contact AFM mode. Veeco Phosphorus (n)-doped silicon contact

metrology probes, model MPP-31123-10 with Al reflective coating and a symmetric tip were used. The nominal width, length and thickness of these rectangular shaped cantilevers were 35 mm, 450 mm and 4 mm, respectively. The nominal force constant of the cantilevers used was 0.9 N/m, and the resonance frequency was 20 kHz. The thickness of the aluminium reflective coating on the backside of the cantilever was 40 nm. The front side of the cantilever was not coated.

AFM images were created and analysed using two software packages: Image Processing and Data Analysis Version 2.1.15 and SPMLab Analysis software from VEECO DI SPMLab NT Ver. 6.0.2. Using the Line Measure tool of the SPMLab Analysis software, the sample profiles were studied along specific directions.

### 3. Results & discussion

#### 3.1 Oil shale bioleaching characteristics of the two strains of *At. ferrooxidans*, A and B

This study visually documented the “phases” of oil shale bioleaching by two different strains of *At. ferrooxidans*. The bioleaching characteristics of oil shale inoculated with bacteria and the sterile control in flasks are shown in Fig. 2. No significant leaching of iron into solution was seen in the abiotic control. The results show that the percentage of bioleached pyrite increased over the duration of the experiment, and *At. ferrooxidans* A significantly promoted the leaching process, with 6.6% of the pyrite bioleached after 120 h compared to 4.1% of pyrite leached by *At.*

*ferrooxidans* B (Fig. 2A). During the process, the pH decreased rapidly, especially at the early stage of leaching, and at 120 h, the pH values reduce to approximately 2.0 for *At. ferrooxidans* A and 2.2 for *At. ferrooxidans* B (Fig. 2B). Changes in the pH and the percentage of bioleached pyrite result from conversion of sulphides to sulphuric acid and the bioleaching of iron from pyrite and are characteristic of the pyrite bioleaching process [34].

Changes in the concentrations of  $\text{Fe}^{2+}$  and  $\text{Fe}^{3+}$  ions in solution are shown in Figure 3. In the control, the amount of  $\text{Fe}^{2+}$  ions was very low and did not increase significantly over time. The concentration of  $\text{Fe}^{3+}$  ions did not change, demonstrating that  $\text{Fe}^{2+}$  oxidation to  $\text{Fe}^{3+}$  proceeded slowly in the

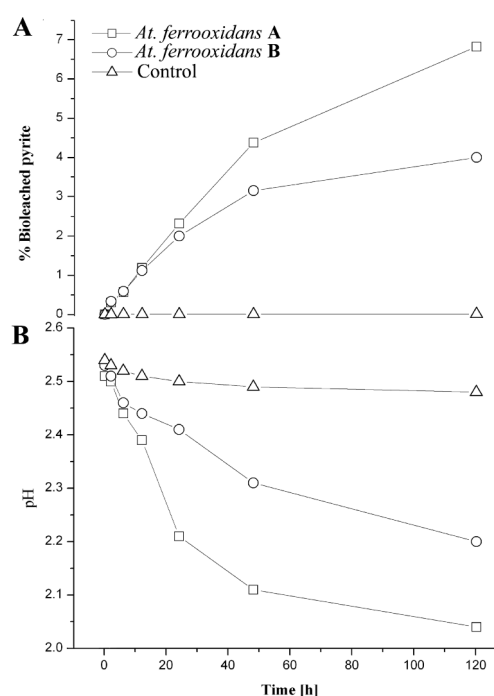


Fig. 2. Changes in the percentages of bioleached pyrite (calculated from total Fe concentration) (A), and pH values (B) over five days, as indicators of bacterial activity.

absence of  $\text{Fe}^{2+}$ -oxidising microbes, despite the low initial pH. In both microbe-inoculated tests, during the first 48 h, the concentration of  $\text{Fe}^{2+}$  increased faster than  $\text{Fe}^{3+}$  but then slowed. The oxidation rate of  $\text{Fe}^{2+}$  indicates that the oxidation activity of *At. ferrooxidans A* is higher than that of *At. ferrooxidans B*.

The amount of leached metal is significantly higher in both of the bacterial cultures than in the abiotic control.

Because the bioleaching profile of the abiotic control did not exhibit significant changes in any of parameters monitored, despite the initial low pH value (pH 2.5), it is evident that the bacteria were responsible for the increased rate of pyrite dissolution beyond what was achieved by chemical dissolution under the same conditions.

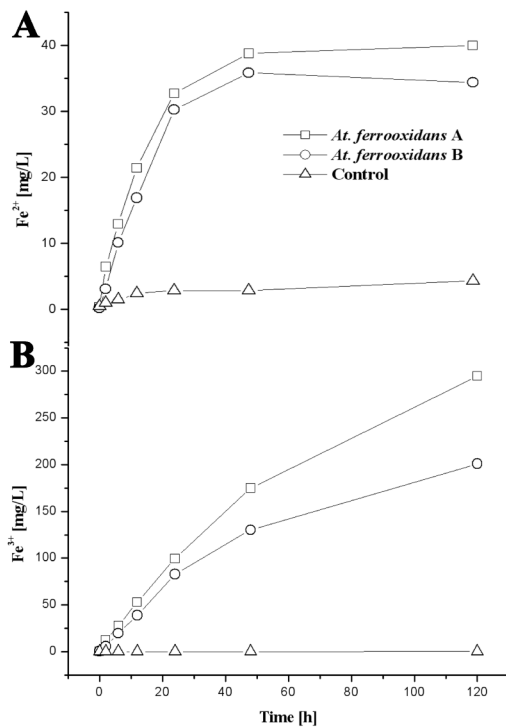


Fig. 3. Changes in the concentrations of  $\text{Fe}^{2+}$  and  $\text{Fe}^{3+}$  in solution throughout the experiments

### 3.2 Visualising the bioleaching mechanism using AFM

Bacteria attached to an oil shale surface were visualised using AFM images taken using the contact mode in air.

The process of oil shale layer colonisation was analysed after incubation of the oil shale samples in the microorganism cultures for 2 h, 6 h, 12 h, 24 h, 48 h and 5 d. It was found that the strain isolated from the Aleksinac copper mine, *At. ferrooxidans A*, had already attached to the shale after two hours and demonstrated a stronger affinity for oil shale, as it attached to the entire shale surface. It is likely that this is because this sediment is an indigenous substrate for these bacteria (Fig. 4).

High numbers of attached cells were visible after 48 h for both samples, with *At. ferrooxidans A* forming bacterial exopolymeric microcapsules surrounding the cells present on the ore surface as well as those in crevices and pits. We assume that the deposited material covering the bacteria is EPS. In this way, these bacteria are forming a biofilm of cells immersed in an exopolymeric matrix.

We assume that these bacteria have developed a special mechanism for attaching to the entire surface because oil shale is a native substrate for this strain.

Bacteria from the Bor copper mine, *At. ferrooxidans B*, demonstrated a lower affinity for attachment to the shale surface. Attachment of this strain to the surface is only visible after 12 hours of incubation, with the bacteria attaching preferably to surface defects, such as cuttings, bumps and niches. After 48 h, there are numerous cells attached to surface defects, with very few

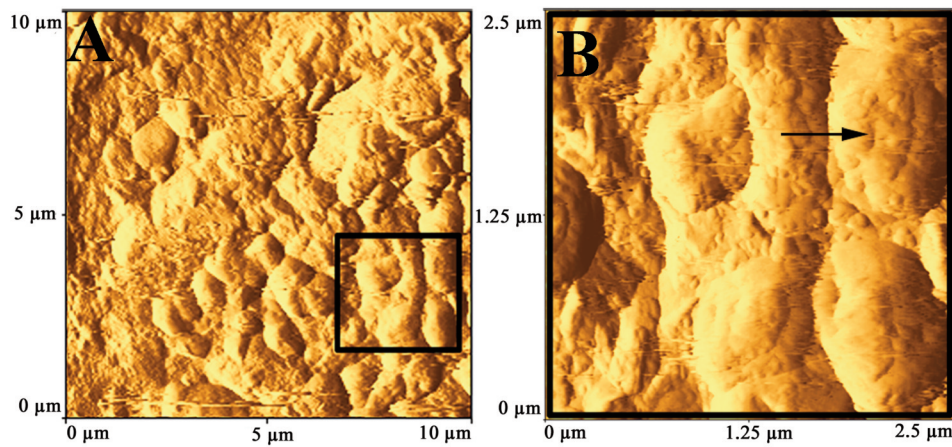


Fig. 4. AFM images of *At. ferrooxidans* A cells attached to an oil shale layer after 48 h of incubation. Vertical deflection images of AFM scans acquired by contact mode in air. Panel (A) shows cells attached all over the surface, and panel (B) represents a close-up view of the framed section on panel (A). The cells are seen as convex ellipsoid shapes, such as the one indicated by an arrow in the topography image in panel (B).

cells observed in other parts of the oil shale layers (Fig. 5). These defects represent sites with bare pyrite emerging from organic surfaces, and the *At. ferrooxidans* B strain prefers these locations because pyrite is the natural substrate for these bacteria.

After 5 days of incubation with the *At.*

*ferrooxidans* A strain, AFM images revealed ellipsoid etched pits (internal diameters of approximately 2 μm) that penetrated the mineral to varying depths. In Fig. 6A, the horizontal cross section AB shows the width of one of the lower regions, which agrees with the microbe dimensions (cross section

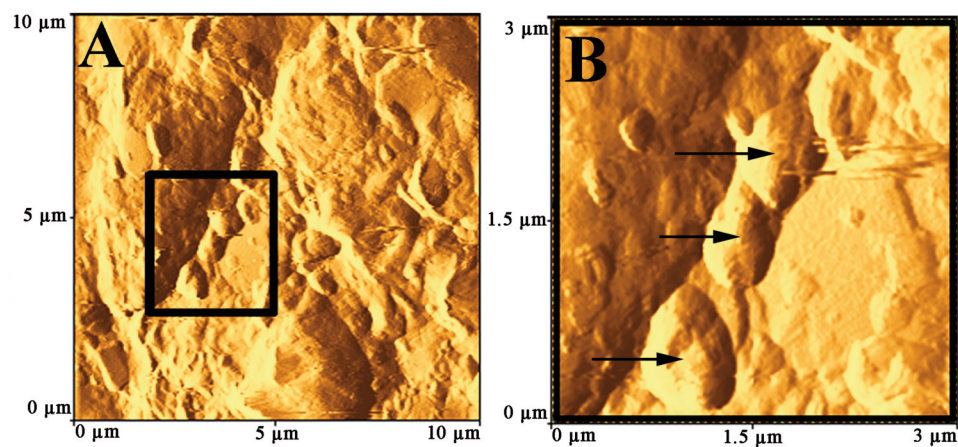


Fig. 5. AFM images of *At. ferrooxidans* B cells attached to oil shale cuttings after 48 h of incubation. Vertical deflection images of AFM scans acquired by contact mode in air. Panel (A) shows an oil shale layer with cells attached to surface defects, and panel (B) represents a close-up view of one cutting, framed on panel (A). The cells are seen as convex ellipsoid shapes, such as the ones indicated by arrows in the topography image in panel (B).

CD, Fig. 6B). This AFM analysis indicates that etched pits represent footprints left by formerly attached cells.

The horizontal cross section EE' of a topographic AFM image of *At. ferrooxidans* A (Fig. 6B) reveals bacterial exopolymeric microcapsules, probably EPS, surrounding the cells. AFM visualisation of EPS surrounding *At. ferrooxidans* cells on solid surfaces has been reported before [35,36].

In our study, bacterial EPS has been visualised on an oil shale surface. The important role of EPS in bacterial attachment and the natural immobilisation of sessile bacterial cells is, observed for the first time for an oil shale substrate.

Thus far, mechanical contact and bioleaching interaction between oil shale and bacteria has not been visualised under physiological conditions. Previous studies used powdered shale and did not investigate the bacterial attachment process [37].

Our experimental system did not contain small quantities of  $\text{Fe}^{2+}$  in the media that would be sufficient for initial oxidation and  $\text{Fe}^{3+}$  formation [38]. Nevertheless, an increase in the iron concentration in solution after only a few hours was observed in our bacterial systems. During the same time, the first cells attached to the oil shale substrate surface. These results indicate that this initial increase in iron concentration is a result of bacteria attaching (adsorbing) to oil shale substrate surface.

The majority of  $\text{Fe}^{2+}$  ions were formed within the first 48 h by microorganisms, after which these ions were oxidised to  $\text{Fe}^{3+}$  ions. During this phase, bacterial cells exhibit the largest affinity for attachment to the substrate surface, with

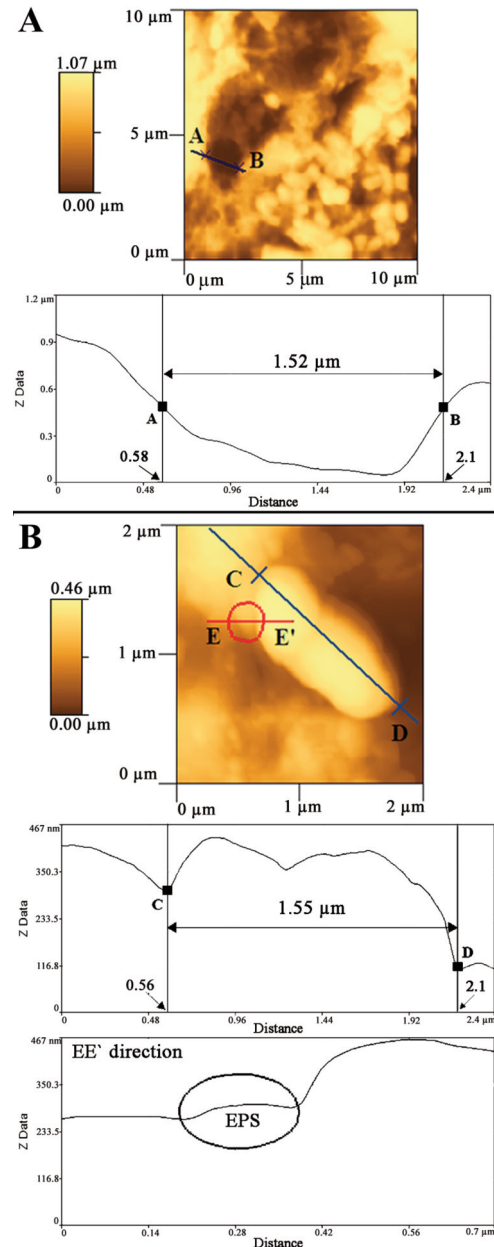


Fig. 6. AFM analysis of the oil shale surface after five days of incubation with *At. ferrooxidans* A. Panel (A) shows a topographic AFM image of the oil shale with one of the pits measured (cross section AB). Panel (B) shows a topographic AFM image of a single *At. ferrooxidans* A cell with the cell width measurement (cross section CD). In addition, AFM analysis demonstrates the existence of EPS surrounding the cell (cross section EE').



*At. ferrooxidans* A forming a biofilm and *At. ferrooxidans* B preferably attaching to cuttings, niches and other defects in the shale surface, which are locations that display bare pyrite on their surfaces. This difference comes from the fact that this shale is the native substrate for *At. ferrooxidans* A, while *At. ferrooxidans* B was isolated from the surface of bare pyrite originating from the copper mine in Bor.

In the next phase,  $\text{Fe}^{3+}$  is used as an oxidising agent in pyrite leaching, leading to a further increase in  $\text{Fe}^{2+}$  levels, which is going to be again bacterially oxidised to  $\text{Fe}^{3+}$  and close  $\text{Fe}^{2+}/\text{Fe}^{3+}$  cycle. At this stage, cells are detaching from the oil shale surface, with free cells beginning to oxidise the  $\text{Fe}^{2+}$  in the solution, regenerating the oxidising agent ( $\text{Fe}^{3+}$ ) for the bioleaching of pyrite. In addition, due to the increase in the  $\text{Fe}^{2+}$  concentration, *At. ferrooxidans* A cells detach from the oil shale surface, and  $\text{Fe}^{2+}$  is converted to  $\text{Fe}^{3+}$  by free cells in solution. As a consequence of the detachment of these cells from the surface of the shale, in the images taken after 5 days, etched pits can be seen in the substrate surface that correlate with bacterial cell dimensions, which suggests that leaching requires an initial attachment of cells to the surface, while in the later stages, once the necessary concentration of iron in the solution is reached, leaching continues by regenerated  $\text{Fe}^{3+}$  as oxidizing agent. Cells now use  $\text{Fe}^{2+}$  instead of iron from pyrite because in terms of energy, this is the more efficient process. A systematic overview of pyrite bacterial leaching is shown in Fig. 7.

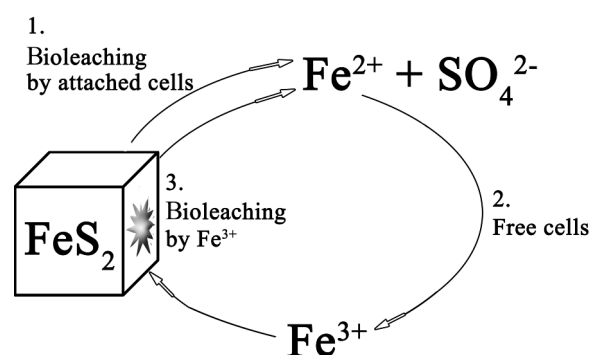


Fig. 7. Systematic overview of pyrite bacterial leaching. 1. In the first stage, cells attach to the surface and  $\text{Fe}^{2+}$  ions are leached into the solution. 2. In the second stage, the number of free cells increases due to the rise in  $\text{Fe}^{2+}$  levels in the solution. 3. In stage 3, bioleaching by  $\text{Fe}^{3+}$  ion as an oxidising agent predominates.

#### 4. Conclusion

By combining AFM surface imaging and leaching analysis following bacterial colonisation of oil shale layers, this study demonstrates that an initial attachment i.e. mechanical contact to the surface is necessary for the leaching and that later on, once a sufficient concentration of  $\text{Fe}^{2+}$  ions in the solution is achieved, cells detach to become free cells, and leaching occurs primarily by the  $\text{Fe}^{3+}$  ions.

Individual bacterial strains are unique, and it is difficult to draw a generalised conclusion about attaching *At. ferrooxidans* to oil shale surface. However, this experiment confirms the hypothesis that microorganisms isolated from sites in which a particular substrate is found will demonstrate stronger binding to that substrate. In this case, thionic bacteria from Aleksinac mines live on oil shale pyrite and

have developed systems for attachment to the shale surface. Attachment is facilitated by the extracellular polymeric substances, which render the non-polar surface more polar and allow for water penetration, promoting the attachment of *At. ferrooxidans* cells. In the experiments using bacterial strains isolated from AMD waters from Bor copper mines, the cells only attached to cuttings and niches where the pyrite was presented at the surface of the oil shale. Five days later, these bacteria did not detach from the oil shale surface, which confirms that bioleaching processes are slower when the bacterial strains are not native to the tested substrate.

### Acknowledgments

*This paper was supported in part by the Ministry of Science and Technological Development of the Republic of Serbia (Project No. III43004), for which we would like to express our gratitude.*

### References

- [1] K. Brendow, Oil Shale, 26 (2009) 357.
- T.F.Yen, in: Oil Shale (T.F.Yen, G. V.Chilingarian,), Elsevier, Amsterdam, 1976, p.129.
- [2] O.Cvetkovic, V.Dragutinovic, M.M.Vrvic, J.A.Curiale, M.Ercegovac, D.Vitorovic, Org. Geochem., 20 (1993) 57.
- [3] V.P.Beškoski, J.Milić, B.Mandić, M.Takić, M.M.Vrvić, Hydrometallurgy, 94 (2008).
- [4] V.P. Beškoski, V.F. Matić, J.Milić, D.Godjevac, B.Mandić, M.M.Vrvić, J. Serb. Chem. Soc., 72 (2007) 533.
- [5] M.M.Vrvić, J. Vučetić, D.Vitorović, Recent Progress in Biohydrometallurgy, Associazione Mineraria Sarda, Iglesias, Italy, 1983, p.527.
- [6] V. Dragutinovic, M.M. Vrvic, O. Cvetkovic, J. Vucetic, D. Vitorovic, J. Serb. Chem. Soc., 64 (1997) 343.
- [7] K. Jasper, B.M. Krooss, G. Flajs, Chr. Hartkopf-Froder, R. Littke, Int. J. Coal. Geol., 80 (2009) 1.
- [8] M. Sert, L. Ballice, M. Yuksel, M. Saglam, Oil Shale 26 (2009) 463.
- [9] A. Turan, O. Yucel, J. Min. Sect. B-Metall., 47 (2011) 219.
- [10] D.E. Rawlings, Microb. Cell Fact., 4 (2005) 1.
- [11] N.J. Coram, D.E. Rawlings, Appl. Environ. Microbiol., 68 (2003) 838.
- [12] N.Okibe, M.Gericke, K.B.Hallberg, D.B.Johnson, Appl. Environ., Microbiol. 69 (2003) 1936.
- [13] M.A.Ghauri, N.Okibe, D.B.Johnson, Hydrometallurgy, 85 (2007) 72.
- [14] W. Zeng, G. Qiu, H. Zhou, X. Liu, M. Chen, W. Chao, C. Zhang, J. Peng, Hydrometallurgy 100 (2010) 177.
- [15] Y. Jiao, G.D. Cody, A.K. Harding, P. Wilmes, M. Schrenk, K.E. Wheeler, J.F. Banfield, M.P. Thelen, Appl. Environ. Microbiol., 76 (2010) 2916
- [16] Y.Q. Li, D.S. Wan, S.S. Huang, F.F. Leng, L. Yan, Q. Ni, H.Y. Li, Curr. Microbiol. 60 (2010) 17.
- [17] R. Yu, Y. Ou, J. Tan, F. Wu, J. Sun, L. Miao, D. Zhong, Trans. Nonferrous Met. Soc. China 21 (2011) 407
- [18] B. Vu, M. Chen, R.J. Crawford, E.P. Ivanova, Molecules, 14 (2009) 2535.
- [19] A. Vilinska, K.H. Rao, Geomicrobiology Journal, 28 (2011) 221.
- [20] A. Turan, O. Yucel, J. Min. Metall. Sect. B-

- Metall. 47 (2011) 219.
- T. A. Fowler, P. R. Holmes, F. K. Crundwell, *App. Environ. Microbiol.*, 65 (1998) 2987.
- [21] M. Song, D. Zhang, *Miner. Eng.*, 22 (2009) 550.
- [22] E.T. Pecina, M. Rodriguez, P. Castillo, V. Diaz, E. Orrantia, *Miner. Eng.*, 22 (2009) 462.
- [23] M.N. Chandrababha, K.A. Natarajan, P. Somasundaran, *Int. J. Miner. Process.*, 75 (2005) 113.
- [24] X. Xie, S. Xiao, J. Liu, *Curr. Microbiol.*, 59 (2009) 71.
- [25] B. Florian, N. Noel, W. Sand, *Miner. Eng.*, 23 (2010) 532.
- [26] J. Lamovec, V. Jovic, M. Vorkapic, B. Popovic, V. Radojevic, R. Aleksic, *J. Min. Sect. B-Metall.*, 47 (2011) 53.
- [27] V.J. Morris, A.R. Kirby, A.P. Gunning, *Atomic Force Microscopy for Biologists*, Imperial College Press, London, 2004.
- [28] M.M. Vrvic, V. Djordjevic, O. Savkovic, J. Vucetic, D. Vitorovic, *Org. Geochem.*, 13 (1988) 1109.
- [29] U. Langer, L. Bohme, F. Bohme, *J. Plant Nutr. Soil Sci.*, 167 (2004) 267.
- [30] V. Beškoski, *Magister thesis (in Serbian)*, Belgrade University, Belgrade, Serbia, 2006.
- [31] D.B. Johnson, S. Rolfe, K.B. Hallberg, E. Iversen, *Environ. Microbiol.* 3 (2001) 630.
- [32] M.P. Silverman, D.G. Lundgren, *J. Bacteriol.*, 77 (1959) 642.
- [33] C.H. Collins, P.M. Lyne, J.M. Grange, J.O. Falkinham III, In *Collin & Lyne's Microbiological Methods*, 8th ed., Arnold, London, 2004 p.144.
- [34] S.Y. Chen, J.G. Lin, *Chemosphere*, 44 (2001) 1093.
- [35] S. Mangold, K. Harneit, T. Rohwerder, G. Claus, W. Sand, *Appl. Environ. Microbiol.* 74 (2008) 410.
- [36] S. Mangold, M. Laxander, K. Harneit, T. Rohwerder, G. Claus, W. Sand, *Hydrometallurgy*, 94 (2008) 127.
- [37] O. Cvetković, M.M. Vrvic, V. Dragutinović, D. Vitorović, *Mikrobiologija (Belgrade)*, 43 (2006) 41.
- [38] S. Wang, G. Zhang, Q. Yuan, Z. Fang, C. Yang, *Hydrometallurgy*, 93 (2008) 51.